Mass-loss of hot stars studied with spectropolarimetric interferometry (SPIN)

Olivier Chesneau, S. Wolf, Karine Rousselet-Perraut, Denis Mourard, Chantal Stehle, et al.

Olivier Chesneau, S. Wolf, Karine Rousselet-Perraut, Denis Mourard, Chantal Stehle, Farrokh Vakili, "Mass-loss of hot stars studied with spectropolarimetric interferometry (SPIN)," Proc. SPIE 4843, Polarimetry in Astronomy, (14 February 2003); doi: 10.1117/12.458618

SPIE.

Event: Astronomical Telescopes and Instrumentation, 2002, Waikoloa, Hawai'i, United States

Mass-loss of hot stars studied with Spectro-Polarimetric Interferometry (SPIN)

O. Chesneau[a], S. Wolf[b], K. Rousselet-Perraut[c], D. Mourard[d], C. Stehle[e], and F. Vakili[f]

[a]Max-Planck-Institut für Astronomie Königstuhl 17, G-69117 Heidelberg, Germany
[b]California Institute of Technology, 1200 E California Blvd.,
Mail code 220-6, Pasadena, CA 91125, USA
[c] Laboratoire d'Astrophysique de l'Observatoire de Grenoble (LAOG)
B.P. 53, F-38041 Grenoble Cedex 9, France
[d] Observatoire de la Côte d'Azur, F-06460 Saint Vallier de Thiey, France
[e] Observatoire de Paris, LUTH, FRE 2462 CNRS,
5 Place Jules Janssen, F-92195 Meudon, France
[f] Universite de Nice Sophia-Antipolis UFR Faculte des Sciences
Parc Valrose F-06108 Nice Cedex 02, France

ABSTRACT

We describe the prospective work undertaken on an interferometric technique using polarimetry called SPIN (Spectro-Polarimetric INterferometry). The polarizing phenomena described in this work have to be taken into account by any stellar interferometer in order to control the fringe signal. Adding a polarimetric device at their combined focus represents no technical difficulty. The use of SPIN can extend interferometry by an important complementary tool for locating and quantizing the mass loss from early type stars since these stars are subject to strong Thomson scattering in their vicinity. As an illustration of the potential of SPIN, we present the results of Monte-Carlo simulations showing the expected signal for realistic hot star environment. Radiative winds ranging from A supergiants to earliest O stars are considered. In particular, the results show the strong expected signal from spherical winds for which no detection of polarization is achievable by classical technics.

Keywords: Polarimetry, long baseline interferometry, hot stars

1. INTRODUCTION

Mass-loss is an intrinsic characteristic of hot stars which eject a strong wind during their whole short life. Despite a great wealth of studies, the origin of this phenomenon remains poorly understood mainly due to the difficulties of classical observational techniques to spatially localize the multiple manifestations of mass-loss events. Without spatial resolution, spectro-polarimetry represents one of the best suited techniques to study mass-loss as the light from the central star can be strongly polarized by its circumstellar environment, mainly by Thomson scattering.

The young technique of optical interferometry has proved its efficiency to study and even monitor Be star disks[1–4] and the environment of the LBV P Cyg.[5] For all these examples, spectro-polarimetry has brought a complementary information of great interest, but the interpretation remained limited by averaging the polarized information over the field of view and any observation of nearly symmetrical object provide an almost undetectable signal. Within this context, it is very attractive to equip a long baseline interferometer with a polarimetric mode.

Such attempts have been performed since the very beginning of interferometry. The unique Narrabri intensity interferometer was used with a polarimeter in 1974 to give an estimate of the polarization-dependent

(Send correspondence to O. Chesneau)
E-mail: chesneau@mpia-hd.mpg.de, Tel: +49 6224 528 215

Polarimetry in Astronomy, Silvano Fineschi, Editor, Proceedings of SPIE
Vol. 4843 (2003) © 2003 SPIE · 0277-786X/03/$15.00

diameter change of β Orionis,[6] but the signal-to-noise ratio (SNR) limitations were well above the expected signal. The experiment was repeated in 1981 with the I2T interferometer on α Lyrae,[7] and in 1997 with the GI2T on the Be star γ Cassiopeiae.[8] These observations showed that instrumental polarization has to be carefully studied and controlled[8] and the accuracy, and thus SNR requirements, are critical as the expected signal is faint. For an extensive presentation of the state of art of SPIN (Spectro-Polarimetric INterferometry), we refer to Rousselet-Perraut et al., these proceedings.

The first theoretical studies on SPIN were performed parallel to the Narrabri Interferometer experiment. Cassinelli & Hoffman[10] investigated the consequences of Thomson scattering around hot stars on the diameter measurements in linearly polarized light (with a single baseline). In the outer regions of the star, the scattered light becomes strongly polarized in a plane perpendicular to the direction of polarization. Owing to the spherical symmetry of the photosphere, the local polarization integrated over the apparent disk cancels out, and no net polarization can be observed by classical spectro-polarimetric technics (i.e., without spatial resolution). In contrast to this, an interferometer in polarization mode can detect a signal due to its sensitivity to the polarized flux in a preferred direction. The star appears smaller in the plane of polarization parallel to the baseline than in the plane perpendicular to it. Rousselet-Perraut[11] performed a theoretical study of the SPIN observables with of a crude model of spherical and elliptical scattering environments. The author also presents an adapted methodology mandatory for such an observational task which is coherent with the results presented in this paper.

2. THE MONTE-CARLO CODE

2.1. Presentation

The simulation of visibilities and polarimetric observables are based on radiative transfer simulations performed with the Monte-Carlo radiative transfer code MC3D (Wolf et al.[12]; see also Wolf et al.,[13] Wolf & Henning[14]). We assume a spherical, extended star which radiates isotropically, i.e., the radiation characteristic at each point of the stellar surface follows the standard cosine law. The radiation field of the star is partitioned into "weighted photons" each of which is characterized by its wavelength and Stokes parameters. The interaction of the stellar photons with the surrounding electron envelope is described by Thomson scattering. Due to (multiple) scattering events the polarization state of the initially unpolarized photons is modified. In order to derive spatially resolved images of the I, Q, and U Stokes vector components of the configuration, photons leaving the electron envelope are projected onto observing planes oriented perpendicular to the path of the photons. Since the optical depth in the electron envelope is $\ll 1$, the enforced scattering concept introduced by Cashwell & Everett[15] was applied in order to achieve a high signal-to-noise ratio for the simulated images within a reasonable computing time. For a more extensive presentation of this code, we refer to Wolf, Henning, & Stecklum, these proceedings.

2.2. Limits

In this study, we consider the flux emitted isotropically by the source. Cassinelli & Hoffman[10] demonstrated that the flux in an extended atmosphere is strongly radially oriented so that the dilution of the polarization due to the finite size of the star is lowered. Thus, in case of dense winds or supergiant stars (Sect 3.1), we underestimate the local polarization at the "photosphere" and within the first few stellar radii where the apparent disk of the star is non-negligible. In further studies, this effect will be partially taken into account.
Another important limitation is that our Monte Carlo radiation transfer code determines the polarization due to multiple photon scattering by dust grains, but does not include the effects of continuous hydrogen absorption and emission seen in disk-like circumstellar envelopes for example. Consequently, our modelling of a hydrogen disk in Sect 3.2 results in an upper limit for the expected interferometric signal from an interferometer, especially for disk studies.

3. VISIBILITY INFORMATION

3.1. Spherical winds

Almost all early-type stars have extended atmospheres and lose mass by a driven wind. In this section, we consider a spherical wind (velocity field), and we apply the following density law:

$$v(r) = v_\infty \left(1 - \frac{r_0}{r}\right)^\beta , \tag{1}$$

where

$$r_0 = R_* \left(1 - \left[\frac{v_0}{v_\infty}\right]^{1/\beta}\right) . \tag{2}$$

In order to illustrate the expected signal from a spherical wind, we modelled the star ζ Puppis (HD 66811), an early O4If supergiant. The simulation parameters are the following:

Distance	D	430 pc
Stellar radius/angular diameter	R_*/Θ	17 $R_\odot$/0.4 mas
Stellar temperature	T_*	42000 K
Mass loss rate	$\dot{M}$	6×10^{-6} $M_\odot$ yr^{-1}
Terminal velocity/beta	v_∞/β	2200 km s^{-1}/1.05
Electronic optical depth	τ_e	0.21

Cassinelli & Hoffman[10] performed a very similar model taking also ζ Puppis as reference. They used a two-component density model for which an extended atmosphere of total thickness τ_e=10 is connected to a flow region with an optical thickness τ_e=0.19, which is close to our parameters. By performing a least-square fit with a uniform disks to the simulated visibilities, they expect a radius ratio between two perpendicular polarization directions of 7%, and the apparent radius from a uniform disk fit of the star emission is 12% larger than the photosphere disk. Our result is more pessimistic since the expected ratio for this model is only 2%, and the apparent radius amounts to 1.05 R_*. The contribution from the extended atmosphere appears to be the largest contribution to the polarized signal.

We have also performed a model of Deneb based on the exhaustive work of Aufdenberg et al..[16] This A supergiant constitutes the cooler spectral type for detection of Thomson scattering in the wind.

Distance	D	685 pc
Stellar radius/angular diameter	R_*/Θ	172 $R_\odot$/2.4 mas
Stellar temperature	T_*	8875 K
Mass loss rate	$\dot{M}$	1×10^{-6} $M_\odot$ y^{-1}
Terminal velocity/beta	v_∞/β	225 km s^{-1}/3
Electronic optical depth	τ_e	0.03

The optical depth due to electron scattering is about 7 times lower than for ζ Puppis, and the expected ratio between two perpendicular directions of polarization does not exceed 0.5%. Also in this case, we expect the results from our Monte-Carlo simulation to be a lower limit of the expected SPIN signal produced in the extended atmosphere of this star, and the radius ratio between perpendicular polarizations can be of the order of 1%. However, it must be pointed out that Deneb's Hα profile exhibits a lack of the broad emission wing seen in the spectra of other supergiants, which are normally attributed to electron scattering.
In natural light we expect that the apparent diameter of Deneb remains identical whatever the baseline direction on the sky. The quasi-sphericity of the envelope is well-established based on the absense of integrated polarization and the absence of detectable variation of radius with baseline for interferometric measurements.[16] Consequently, we expect the same polarized signal from Deneb's wind for different baselines directions.

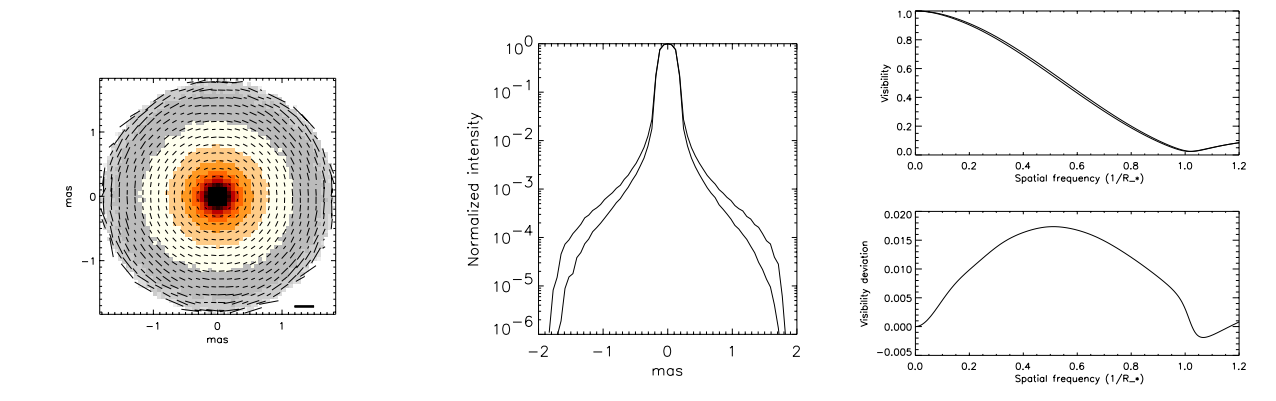

Figure 1. Expected polarization from the ζ Puppis wind model. Close to the photosphere, the wind density strongly decreases following the rapid acceleration modelled by the β law. On the right, the intensity map $I^{\frac{1}{6}}$ (for illustrative purpose) with overplotted polarization is presented (thick bar equal 100% polarization). The flux integrated in the baseline direction for both polarization is plotted in the middle. On the right is showed the visibility signal for both polarization (top), and their difference (bottom).

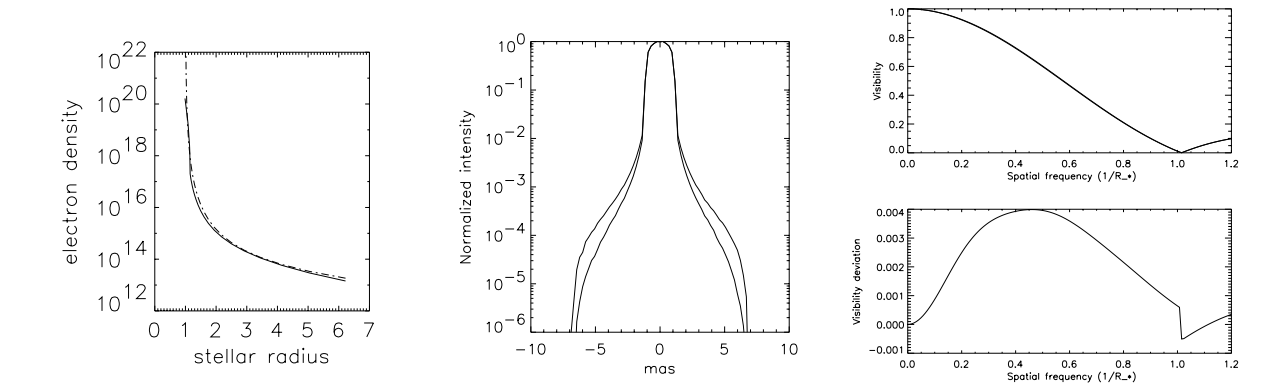

Figure 2. Expected polarization from the Deneb wind model. We have performed a fit of the numerical electron density law from Aufdenberg et al.[16] using the equation (1) (right). The signal expected from this simulation is weak, but still detectable taking into account the brightness of this star.

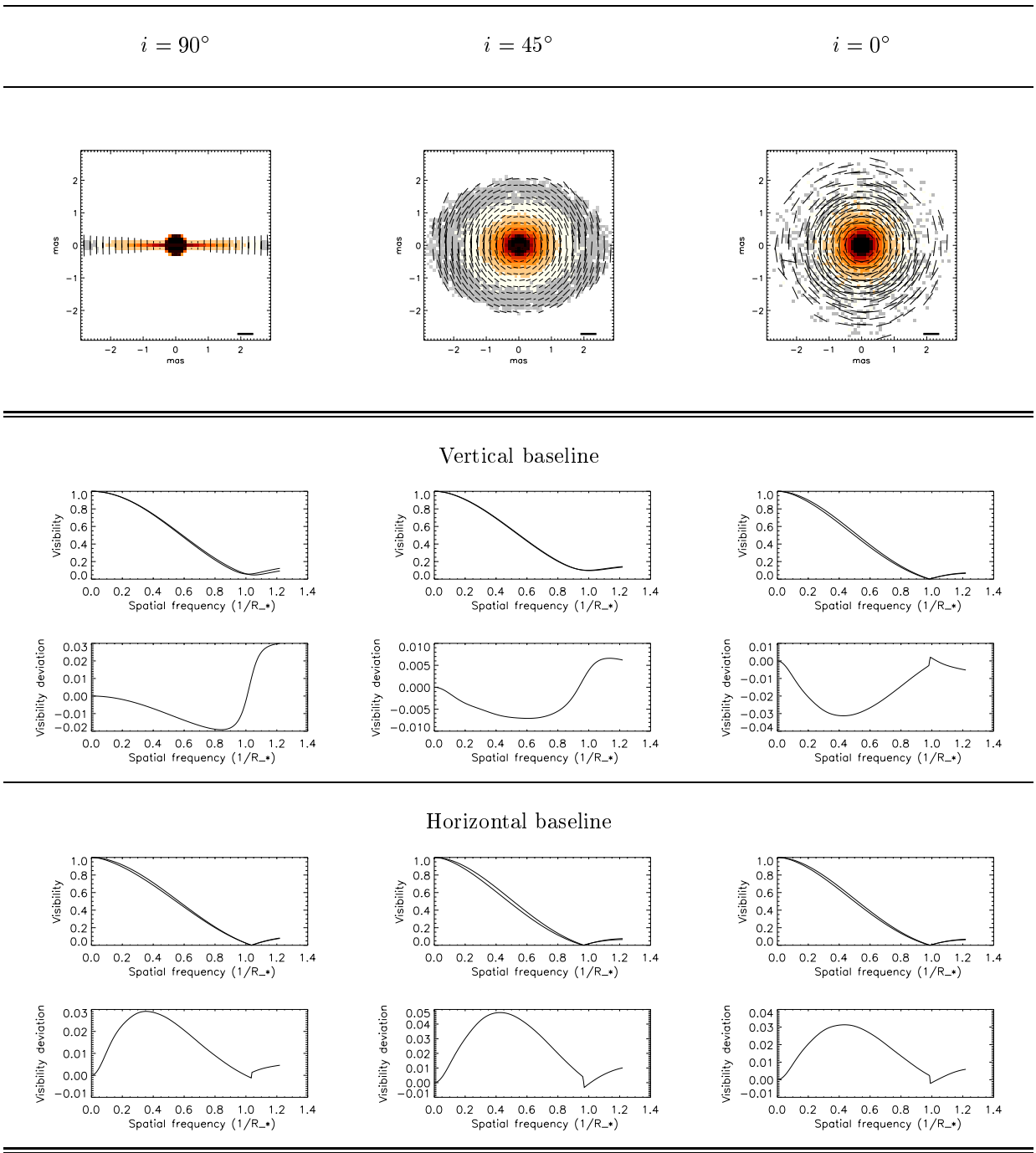

Figure 3. Model of ζ Tau for 3 inclinations corresponding to 3 disk inclinations (columns). The upper subpanels show the intensity maps on the sky with the overplotted polarization P. The thick bar represents a linear polarization of 100%. The lower panels present the overplotted visibility curves for I-Q and I+Q maps, and their difference for a vertical (middle) and horizontal (bottom) baseline orientation. The diffused flux from the envelope is 1.6% ($i = 90°$), 7% ($i = 45°$), and 7.5% ($i = 0°$) of the stellar light.

3.2. Circumstellar disks

Be stars are hot and fast rotating stars surrounded by an extended circumstellar hydrogen envelope. One of the challenging questions on Be stars is the geometry of their disk, and in particular their opening angle, about which there is still an active debate. Most authors have considered geometrically thin disks (half opening angle of 2-5°). Furthermore, interferometric observations have given upper limits of approximately 20° (Quirrenbach et al.[2]). However, the hypothesis of such narrow disks face several problems, and the current set of observations does not provide a unique interpretation on the circumstellar geometry.
The model from Waters[17] has been successfully used to explain the near and far IR observations and is coherent also with polarization data (Coté & Waters,[18] Waters & Marlborough[19]). They model the disk as an equatorial cone with a density law in the form $\rho = \rho_0 r^{-n}$ with the density gradient n ($2 < n < 5$), the density of the disk ρ_0, the disk radius $R_{\rm d}$, the viewing angle i, and the disk half-aperture θ as main parameters. We performed simulations of the polarized emission of Be star disks. These MC3D code simulations have been tested using as reference the work from Wood et al.[20] (Fig. 8). We obtain very similar results for the integrated polarization, (within less than 10%) taken into account that our density law is not exactly similar that used by Wood et al. which allows a colatitude dependency of the density. However, their polar-to-equatorial density ratio of $1 : 10^3$ is very strong, so that we can consider the two models as very close. It must be pointed out that in this study the only emission process considered is the Thomson diffusion.
In particular, we used as template the star ζ Tau (B1 IVe-sh star), which is a well studied case of edge-on Be star ($i \simeq 82°$; Wood et al.[21]). We used a set of parameters close to Wood et al.,[21] i.e., $R_* = 6R_\odot$, $T_* = 2 \times 10^5$ K, and for the the disk simulation, a very thin disk of opening angle of 3°, and density law which defines an optical depth in the disk plane of about $\tau_e = 3$ (density gradient $n = -3$).

In Fig 3 we present the expected interferometric signal for ζ Tau for different inclinations.

Fig. 4 illustrates the differences and the complementarity between the polarimetric and interferometric observables. We reproduce quantitatively the integrated polarization curve from Wood et al..[20] In edge-on view, there is a strong decrease of the local polarization due to the highly optically thick line of sight (multiple scattering). Nevertheless the integrated polarization is compensated by the higher asymmetry of the system (right panel in the figure). We see also that the SPIN signal is still detectable on pole-on view and even slightly larger than at $i = 90°$, the maximum location at $i \simeq 65°$ being equivalent. The interferometer is very sensitive to the large projected emitting surface of the pole-on view which compensates the lower local polarization.

4. GI2T OBSERVING PROGRAM

The GI2T-REGAIN spectro-interferometer is composed of two 1.5-m telescopes which can be displaced on a North-South baseline spanning from 12 to 65m. The REGAIN beam combiner forms the interferometric focus of the instrument. The visible focus is equipped with a dedicated visible spectrograph and two photon counting detectors. A polarimetric mode can be inserted inside the REGAIN spectrograph and is removed (thanks to a motorization) for visibility measurements in natural light. The polarimetric mode of REGAIN includes a quartz Wollaston prism, and an input quarter-wave plate oriented at 45° with respect to Wollaston neutral axes which can be inserted before the Wollaston prism for analyzing and recording the circularly polarized components. To decouple the visibility measurements from the detector response, polarization states are switched. The Wollaston prism can rotate up to 180° (this movement is motorized). For a complete optical scheme, see the Fig. 4 in Rousselet-Perraut et al. (these proceedings).
The data reduction procedure[22] can be applied separately on both images, for independent visibility measurements (amplitude and phase as a function of wavelength). We can also cross-correlate the images in both polarizations for differential measurements. This last procedure appears promising to greatly improve the sensitivity on polarized signal. In any case the data reduction will take into account the observing procedure, which has been defined for calibration and astrophysical purposes.

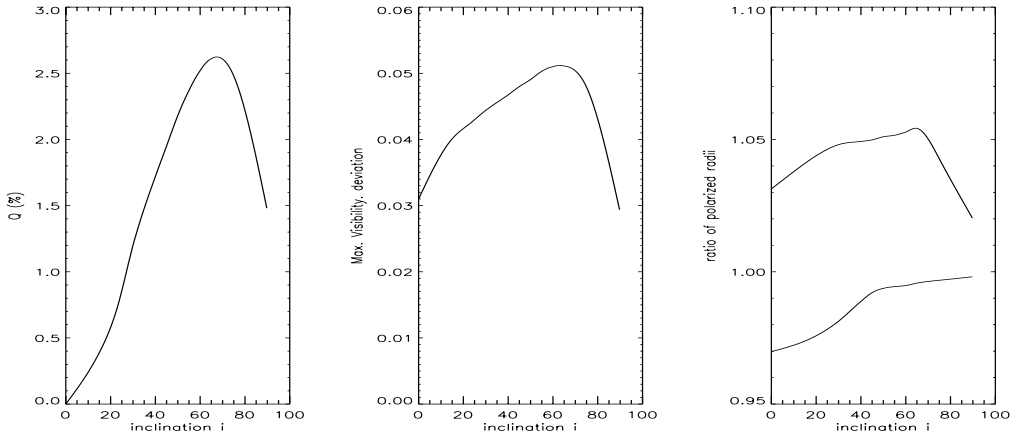

Figure 4. Polarimetric and SPIN signal for various inclinations. In the middle the expected SPIN signal is shown, represented by the maximum of the deviation curve (as show in Fig.1 and Fig.3). On the right the ratio of a uniform diameter (UD) fit on the polarized visibility curves $r = V_{\mathrm{I+Q}}/V_{\mathrm{I-Q}}$ is reported. The upper(lower) curve describes the ratio for an horizontal r_{H}(vertical r_{V}) baseline. Due to the spherical symmetry, the pole-on signal is just inverted between the baseline. At higher inclinations r_{H} increases, but the vertical polarized signal disappears and r_{V} reaches almost 1. The curves are noisy because of the quality of the uniform disk fit.

Name	Distance in pc	Star angular diam. in mas	SPIN amplitude $V_{\parallel} - V_{\perp}$ at $0.5\mu m$	SPIN amplitude $V_{\parallel} - V_{\perp}$ at $0.66\mu m$	Spectral Typ. Comments
γ Cas	190	0.45	0.05-0.06	0.03-0.04	B0 IVe, $i \simeq 45°$
ζ Tau	130	0.4	0.02-0.03	0.015-0.025	B4 IIIpe, $i \simeq 82°$
η Tau	110	0.4	0.03-0.04	0.025-0.03	B7 IIIe, $i \simeq 0°$
Deneb	685	2.4	$\leq$0.01	$\leq$0.01	A2Iae
β Lyr	370	0.2	?	?	B7Ve, $i \simeq 90°$, binary

So far, the simulated polarized signal has no dependence on wavelength. However, neutral hydrogen absorbs some light before and after scattering, and the envelope emission dilutes the polarization. We have corrected semi-quantitatively our signal expectations for Be stars (as presented in Fig.3) by means of the spectro-polarimetric data available for these stars.[23] As an example, the spatially integrated polarization of γ Cas declines from 0.6% at the Balmer jump, to reach 0.52% at 0.5μm, and 0.4% at 0.66 μm. This evolution reflects only the changes in free-bound opacity and free-free emission towards the envelope, and affects the local polarization, and our SPIN signal. We have applied these spectro-polarimetric changes as correcting factor for our estimation of the signal of γ Cas and ζ Tau. For η Tau, only spectro-photometric data have been used because the intrinsic integrated polarization of this star is almost zero due to probably a system inclination close to pole-on.

The optimum baseline is the that for which the visibility is between 0.5 and 0.7. For γ Cas and Deneb, the corresponding baseline range is 20-40m (at $0.66\mu m$ region) and 15-30m (at 0.5 μm) and therefore well within the baseline range of the GI2T (10-60m). For β Lyr, the optimum baseline depends on the complex geometry of this binary star.

4.1. Acknowledgments

The authors thanks J.P. Aufdenberg for having provided a numerical detailed model of Deneb. O.C. is grateful to the "Max-Planck Institut für Astronomie" for a postdoctoral grant. S.W. acknowledges financial supported through the NASA grant NAG5-11645, and through the grant DP.10633 (project 101555).

REFERENCES

1. P. Stee, F. X. de Araùjo, F. Vakili, D. Mourard, L. Arnold, D. Bonneau, F. Morand, and I. Tallon-Bosc, "γ Cassiopeiae revisited by spectrally resolved interferometry.," *A&A* **300**, pp. 219–236, 1995.
2. A. Quirrenbach, K. S. Bjorkman, J. E. Bjorkman, C. A. Hummel, D. F. Buscher, J. T. Armstrong, D. Mozurkewich, I. Elias, N. M., and B. L. Babler, "Constraints on the Geometry of Circumstellar Envelopes: Optical Interferometric and Spectropolarimetric Observations of Seven Be Stars," *ApJ* **479**, p. 477, 1997.
3. F. Vakili, D. Mourard, P. Stee, D. Bonneau, P. Berio, O. Chesneau, N. Thureau, and F. Morand, "Evidence of one-armed oscillations in the equatorial disk of ζ Tau from GI2T spectrally resolved interferometry," *A&A* **335**, 1997.
4. P. Berio, P. Stee, F.Vakili, D. Bonneau, O. Chesneau, N. Thureau, D. L. Mignant, and R. Hirata, "Interferometric insight into γ Cas long-term variability," *A&A* **345**, p. 203, 1999.
5. F. Vakili, D. Mourard, D. Bonneau, F. Morand, and P. Stee, "Subtle structures in the wind of P Cygni.," *A&A* **323**, 1997.
6. R. H. Brown, J. Davis, and L. Allen, "An attempt to detect a corona around β Orionis with an intensity interferometer using linearly polarized light," *MNRAS* **168**, p. 93, 1974.
7. F. Vakili, "Study of Stellar Polarization with the CERGA Interferometer.," *A&A* **101**, 1981.
8. K. Rousselet-Perraut, F. Vakili, and D. Mourard, "Polarization effects in stellar interferometry," *Optical Engineering* **35 (10)**, p. 2943, 1997.
9. K. Rousselet-Perraut, F. Vakili, D. Mourard, F. Morand, D. Bonneau, and P. Stee, "An attempt to detect polarization effects in the envelope of γ Cassiopeiae with the GI2T interferometer," *A&A Sup Ser* **123**, p. 173, 1997.
10. J. Cassinelli and N. Hoffman, "The effect of linearly polarized light from extended stellar atmospheres on interferometer response functions.," *MNRAS* **173**, p. 789, 1975.
11. K. Rousselet-Perraut, "Can interfero-polarimetry constrain extended atmospheres' models?," *A&A Sup Ser* **131**, p. 361, 1998.
12. S. Wolf, "MC3D - 3D Continuum Radiative Transfer, Version 2," *Comp. Phys. Comm.* **in press**, 2002.
13. S. Wolf, T. Henning, and B. Stecklum, "Multidimensional Self-Consistent Radiative Transfer Simulations based on the Monte-Carlo Method," *A&A* **439**, p. 839, 1999.
14. S. Wolf and T. Henning, "Accelerated Self-Consistent Radiative Transfer based on the Monte-Carlo Method," *Comp. Phys. Comm.* **132**, p. 166, 2000.
15. E. Cashwell and C. Everett, *A practical manual on the Monte Carlo Method for random walk problems.*, Pergamon, New York, 1959.
16. J. P. Aufdenberg, P. H. Hauschildt, and E. Baron, "Spectropolarimetric observations of ζ Tau.," *ApJ* **570**, p. 344, 2002.
17. L. Waters, "The density structure of discs around Be stars derived from IRAS observations," *A&A* **162**, 1986.
18. J. Coté, L. Waters, and J. Marlborough, "Be stars with small discs: structure and dynamics," *A&A* **307**, p. 184, 1996.
19. L. B. F. M. Waters and J. Marlborough, "Constraints on Be star wind geometry by linear polarisation and IR excess," *A&A* **256**, 1992.
20. K. Wood, K. Bjorkman, A. Whitney, and A. Code, "The effect of multiple scattering on the polarisation from axisymmetric circumstellar envelopes," *ApJ* **461**, 1996.
21. K. Wood, K. Bjorkman, and J. Bjorkman, "Deriving the Geometry of Be Star Circumstellar Envelopes from Continuum Spectropolarimetry. I. The Case of ζ Tauri," *ApJ* **477**, 1997.
22. D. Mourard, J.-M. Clausse, E. Pedretti, and M. Pierron, "GI2T/REGAIN control system and data reduction package," in *Astronomical Interferometry*, **4006**, SPIE, 2000.
23. D. McDavid, "A useful approximation for computing the continuum polarization of Be stars," *ApJ* **553**, p. 1027, 2001.